

parasitic element for the monopole type patch in the upper frequency band.

In general, an electrically small antenna, such as internal antennas for the mobile handsets, is a support-structure-defined antenna (SSDA), whose electric performances and characteristics are determined by the radiating element itself as well as the shape or size of the support structure [5]. Because its current distribution depends on the location of the feeding and shorting posts as well, the feeding and shorting posts of the proposed antenna are optimized by HFSS simulator.

### 3. SIMULATION AND MEASUREMENT RESULTS

Figure 4 shows that the proposed antenna has sufficient bandwidth for penta-band operation, including the GSM850, GSM900, DCS, PCS, and WCDMA bands, and that its impedance bandwidths ( $VSWR \leq 3$ ) are 27.0% and 67.25% for the GSM and DCS/PCS/WCDMA bands.

The measured far-field radiation patterns of the proposed antenna at 850, 920, 1800, 1900, and 2000 MHz are shown in Figure 5. The measured peak gains are 1.21, 1.67, 1.74, 2.48, and 1.45 dBi for the GSM850, GSM900, DCS, PCS, and WCDMA bands, respectively. The average gains in  $x$ - $y$  plane are 0.17, 0.39,  $-0.34$ , 0.55, and  $-0.42$  dBi at each band, respectively. The overall shape of the radiation patterns and the features of the antenna electrical performance are highly suitable for wireless communication terminals.

### 4. CONCLUSIONS

This letter proposes a monopole type penta-band internal antenna using a parasitic element for covering GSM850, GSM900, DCS, PCS, and WCDMA bands. Especially, wide impedance bandwidth in higher band covering three application bands is obtained. Because the slits positioning around the shorting pin and the feeding pin has an effect on the electrical path of the antenna, it plays important roles in achieving a size reduction. This should be an easy and successful way to deal with problems of the frequency variations when a prototype of an antenna is practically applied for mobile handsets. Because the proposed antenna requires a small size to apply, the antenna is applicable for the mobile handset as internal antenna.

### REFERENCES

1. H.S. Yoon and S.O. Park, A new compact hexaband internal antenna of the planar inverted F-Type for mobile handsets, *IEEE Trans Antennas Propag* 6 (2007), 336–339.
2. P. Salonen, M. Keskilammi, and M. Kivikoski, New slot configurations for dual-band planar inverted-F antenna, *Microwave Opt Technol Lett* 28 (2001), 293–298.
3. F.R. Hsiao, H.T. Chen, G.T. Lee, T.W. Chiou, and K.L. Wong, A dual-band planar inverted-F antenna with a branch-line slit, *Microwave Opt Technol Lett* 32 (2002), 310–312.
4. G.K.H. Lui and R.D. Murch, Compact dual-frequency PIFA designs using LC resonators, *IEEE Trans Antennas Propag* 49 (2001), 1016–1019.
5. S.D.A. Edvardsson, A new family of small antennas used since long time, *IEEE Antennas Propag Symp* (2001), 464–467.

© 2008 Wiley Periodicals, Inc.

## INVESTIGATION ON WIDEBAND DIGITAL FEEDBACK PREDISTORTION TECHNIQUE FOR MOBILE WiMAX MULTICARRIER APPLICATIONS

Jangheon Kim, Junghwan Moon, Jungjoon Kim, Ildu Kim, and Bumman Kim

Department of Electrical Engineering, Pohang University of Science and Technology (POSTECH), Gyeongbuk 790-784, Republic of Korea; Corresponding author: rage3k@postech.ac.kr

Received 2 April 2008

**ABSTRACT:** We have developed a new wideband digital feedback predistortion technique for wideband signals by combining digital feedback predistortion linearization and memory-effect compensation techniques, and investigated linearization performance for 802.16e mobile WiMAX 2FA signal. For this purpose, a 2.655-GHz class-AB amplifier with 170-W peak envelope power is fabricated. The proposed technique is compared with the digital feedback predistortion. We have experimentally demonstrated that the new wideband digital feedback predistortion technique is suitable to linearize amplifiers for mobile WiMAX multicarrier application. © 2008 Wiley Periodicals, Inc. *Microwave Opt Technol Lett* 50: 3048–3052, 2008; Published online in Wiley InterScience (www.interscience.wiley.com). DOI 10.1002/mop.23877

**Key words:** power amplifier; linearization; linearity; WiMAX

### 1. INTRODUCTION

Next-generation systems for wireless communication have been progressed enough to handle a wide range of high data rate signals in multiuser environments with peak data rate, as a target, of up to  $\sim 100$  Mbit/s for high-mobility applications such as mobile access, and up to  $\sim 1$  Gbit/s for low-mobility applications such as nomadic/local wireless access [1]. Among various new communication standards presented in the communication systems, worldwide interoperability for microwave access (WiMAX) standard provides high data rate in both fixed and mobile environments, based on orthogonal frequency division multiple access modulation and straight Internet protocol compatibility. In other words, this WiMAX offers higher capacity and coverage from higher order modulation schemes and wider channel bandwidth [2]. This modulation scheme requires stringent linearity from power amplifiers (PAs) for wide bandwidths and high PAPRs. Thus, it is necessary to apply a digital predistortion (DPD) technique for the wideband signal to achieve the linearity requirement.

As the signal bandwidth increases, PAs exhibit serious memory effects that are defined as the instantaneous nonlinearity depended on not only a current signal but also a past signal. These memory effects cause unbalanced spurious emissions and scattered AM/AM and AM/PM distortions for modulated signals. For this bandwidth-dependent distortion, memoryless DPD techniques can only provide limited linearization. Therefore, the DPD algorithm has to include a memory compensation structure to correct the nonlinearity, and such algorithms have been extensively studied for multicarrier CDMA and WCDMA (Wideband Code Division Multiple Access) applications [3–7].

In our group, the digital feedback predistortion (DFBPD) technique, based on feedback predistortion [8], has been developed. We have presented the DFBPD technique's advantages such as a simple PD algorithm, fast convergence speed, accurate PD signal extraction, and better system tolerance [9, 10]. In order to provide good linearization performance for wideband signals, a wideband DFBPD (WDFBPD) technique including a memory-effect compensation algorithm is proposed [11].

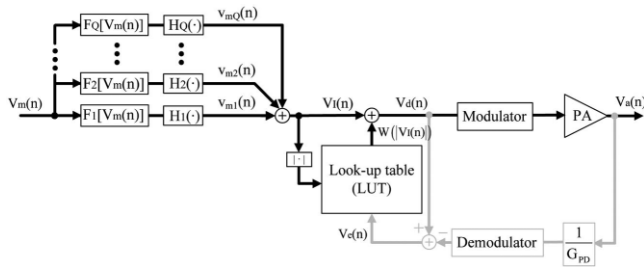
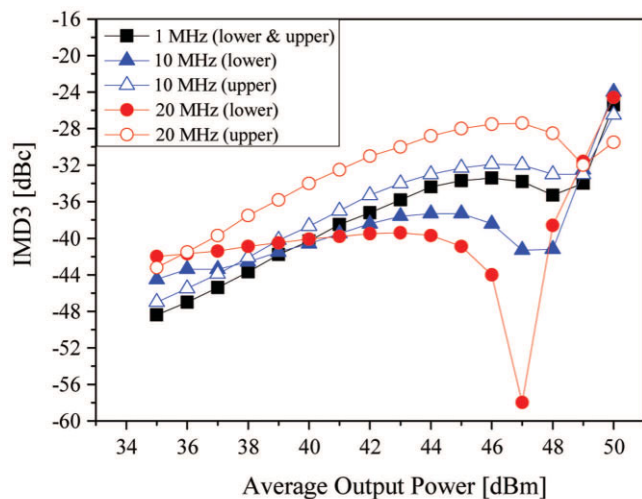
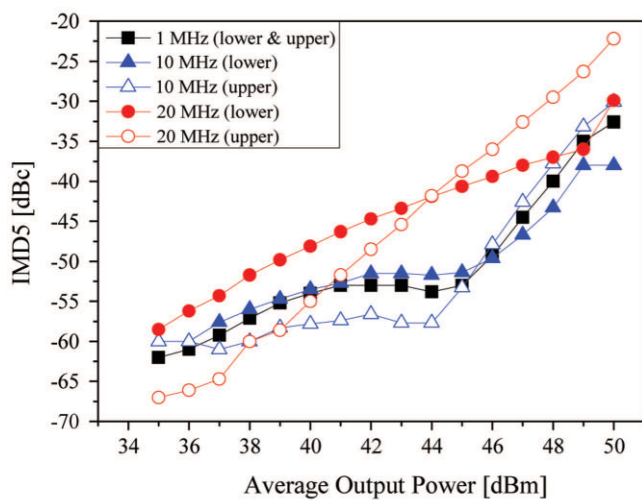


**Figure 1** Simplified block diagram of proposed wideband digital feedback predistorter

The objective of this article is to investigate the WDFBPD technique for 802.16e mobile WiMAX 2FA signal with 20-MHz bandwidth. For this purpose, a class-AB amplifier is fabricated using two LDMOSFETs with 85-W PEP. Before applying the PD algorithm, the nonlinear characteristics and memory effects for two-tone and WiMAX 2FA signals are explored. Based on the



(a)



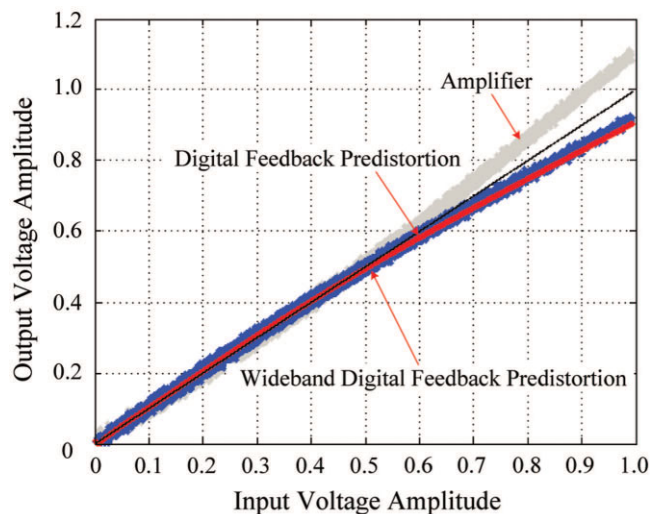
(b)

**Figure 2** Measured (a) IMD3 and (b) IMD5 characteristics for two-tone signals. [Color figure can be viewed in the online issue, which is available at [www.interscience.wiley.com](http://www.interscience.wiley.com)]

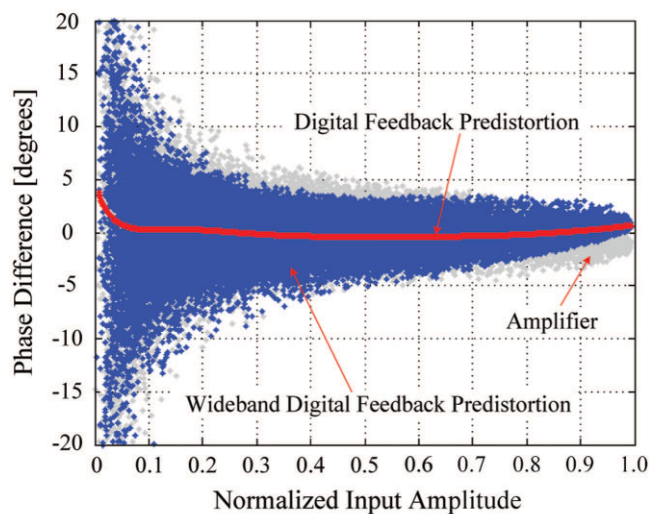
examination, the amplifier is linearized using the WDFBPD algorithm, demonstrating superior linearization performance over the DFBPD algorithm for a wideband signal such as mobile WiMAX multicarrier application.

## 2. OPERATION OF WDFBPD TECHNIQUE

By combining the DFBPD and memory-effect compensation algorithms, a new WDFBPD technique has been developed as shown in Figure 1. This algorithm can linearize memory effects using a simplified memory polynomial structure, because the non-linearity is completely compensated by the DFBPD algorithm. In other words, the WDFBPD algorithm can independently compensate for memory effects and memoryless nonlinear characteristics. The memory compensation structure consists of multiple branches connected in parallel. Each branch is composed of a nonlinear function  $F_q(\cdot)$  and an impulse response  $H_q(\cdot)$ . Here, because the signal caused by memory effects is composed of mixed signals of

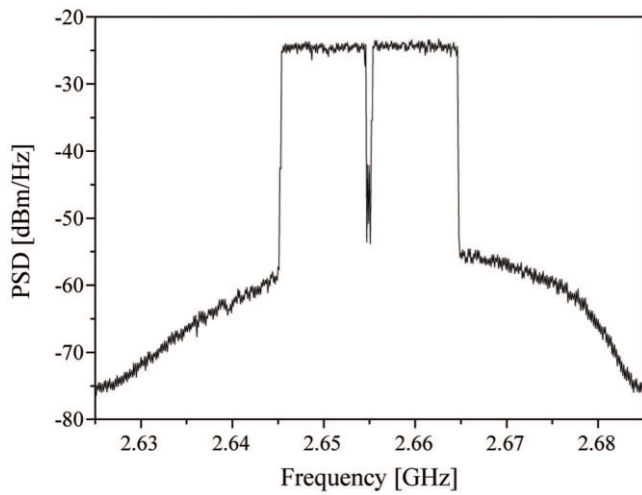


(a)

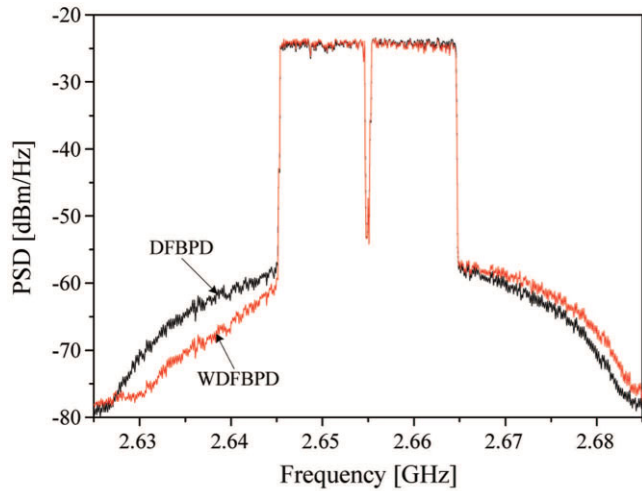


(b)

**Figure 3** Measured predistorted (a) AM/AM and (b) AM/PM characteristics before linearization and after predistortion by the DFBPD and WDFBPD algorithms for the WiMAX 2FA signal. [Color figure can be viewed in the online issue, which is available at [www.interscience.wiley.com](http://www.interscience.wiley.com)]



(a)



(b)

**Figure 4** Measured WiMAX 2FA spectra of (a) amplifier and (b) pre-distorted signals. [Color figure can be viewed in the online issue, which is available at [www.interscience.wiley.com](http://www.interscience.wiley.com)]

not only odd-order, even-order components as well as the fundamental but also past and current signals, the memory compensation structure is a form of the simplified memory polynomial. The memory compensation algorithm transforms the input signal into an inverse envelope memory signal. The inverse signal is added to the LUT error signal before exciting PA. The pre-distorted signal  $V_d(n)$  is expressed as

$$V_d(n) = W(|V_1(n)|) + V_1(n), = W(|V_1(n)|) + \sum_{q=1}^Q \sum_{l=0}^{L-1} a_{lq} V_m(n-l) |V_m(n-l)|^{q-1}, \quad (1)$$

where  $V_m(n)$ ,  $V_1(n)$ , and  $W(|V_1(n)|)$  are the modulated source, inverse scattered, and LUT output signals, respectively. Here,  $a_{lq}$  are coefficients of the impulse response. The parameter  $Q$  specifies the number of the parallel branches and  $L$  is the memory length of the WDFBPD algorithm.

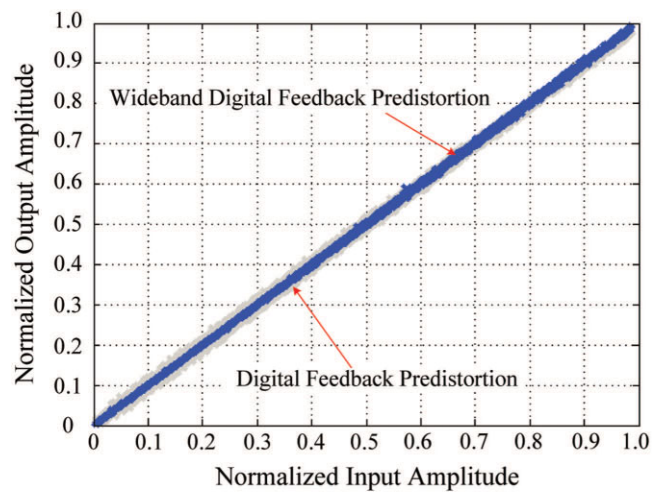
The WDFBPD algorithm process is given as follows: In the first step, the PA is modeled from source and its measured output

signals. In the next step, the pre-distorted signal, which only compensates the memoryless PA nonlinearity, is made using the DFBPD algorithm with the condition of  $Q = 1$  and  $L = 0$  ( $V_m = V_1$ ). In this process, the data in the LUT can be constructed as a function of the input for the training sequence with time samples,  $n = 1, 2, \dots, N$ , at low speed. This algorithm can be written as

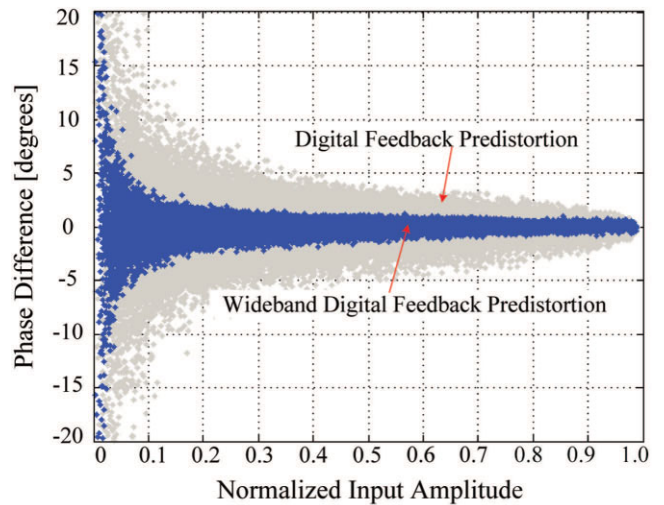
$$W^k(|V_1(n)|) = V_e^{k-1}(n)|_{|V_1(n)|}, = \left[ V_d^{k-1}(n) - \frac{V_a^{k-1}(n)}{G_{PD}} \right] |_{|V_1(n)|}, \quad (2)$$

$$\text{for iteration } k = 1, 2, K \quad (3)$$

where  $V_e^{k-1}(n)$  is the error signal and  $G_{PD}$  is the overall PD system gain. After this procedure, the linearized amplifier input and output data ( $V_m$  and  $V_a$ ) are collected, and the AM/AM and AM/PM characteristics are identified. To compensate the scattering characteristics caused by the memory effects, the coefficients  $a_{lq}$  of the impulse response are solved using the recursive least squares (RLS) algorithm [12]. For the RLS process, the source



(a)



(b)

**Figure 5** Measured (a) AM/AM and (b) AM/PM output characteristics after DFBPD and WDFBPD linearization at an average output power of 42 dBm for the WiMAX 2FA signal. [Color figure can be viewed in the online issue, which is available at [www.interscience.wiley.com](http://www.interscience.wiley.com)]

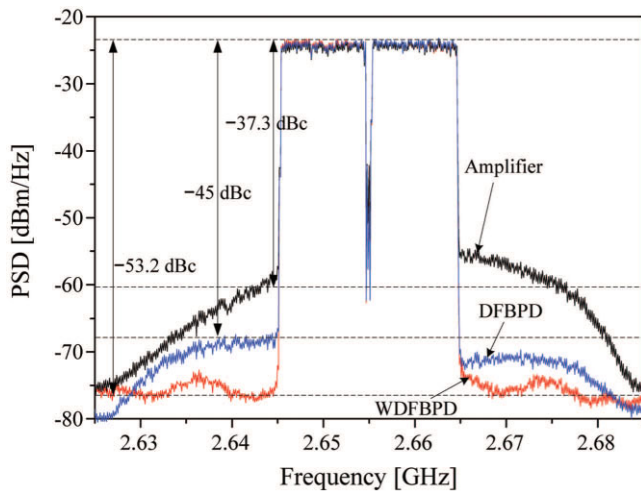


**Figure 6** Measured WiMAX 2FA spectra before and after linearization at an average output power of 42 dBm. [Color figure can be viewed in the online issue, which is available at [www.interscience.wiley.com](http://www.interscience.wiley.com)]

data  $V_m$  and the memoryless nonlinearity correction data  $V_a$  of the training sequence are used. From these data, the scattering test signal  $V_t$  is constructed. If the data are the training sequences with time samples,  $n = L, L + 1, \dots, N$ , then  $V_t$  can be written in matrix format as follows:

$$V_t = UA, \quad (4)$$

where

$$V_t = [V_t(L) V_t(L+1) \dots V_t(n) \dots V_t(N)]^T.$$

$$A = [A_1 A_2 \dots A_Q]^T.$$

$$A_q = [a_{0q} a_{1q} \dots a_{(L-1)q}]^T.$$

$$U = [U_1(n) U_2(n) \dots U_Q(n)].$$

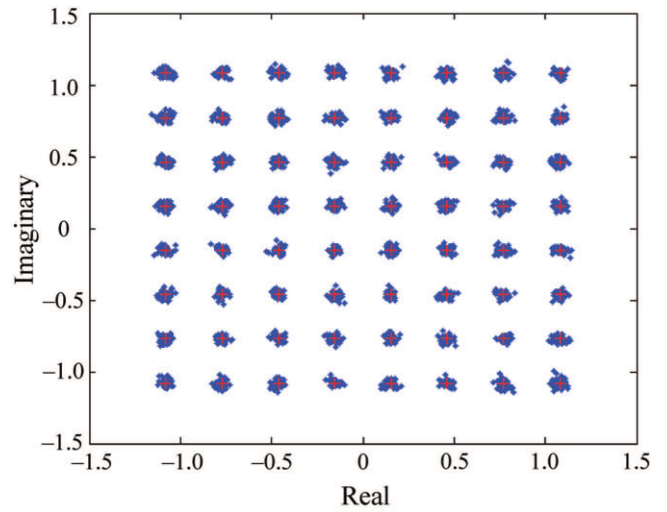
$$U_q(n) = \begin{bmatrix} V_a(n-0) |V_a(n-0)|^{q-1} \\ V_a(n-1) |V_a(n-1)|^{q-1} \\ \vdots \\ V_a(n-L+1) |V_a(n-L+1)|^{q-1} \end{bmatrix}^T.$$

$$q = 1, 2 \dots Q.$$

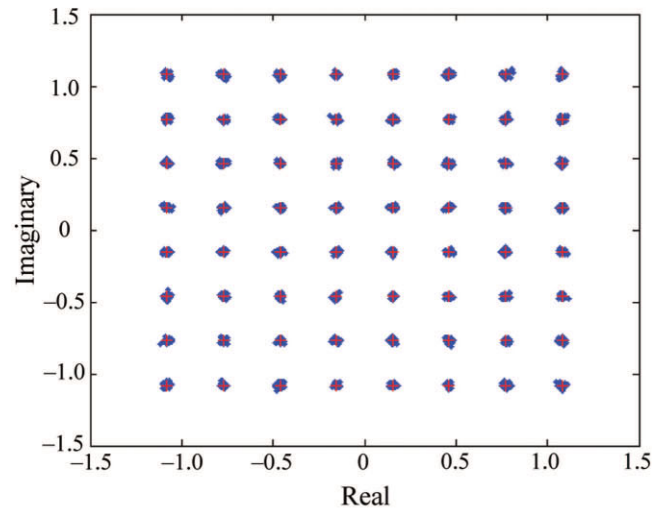
Finally, the linearization for the memoryless nonlinear characteristics and memory effects are accomplished simultaneously by applying the total predistorted signal of (1) to the amplifier.

### 3. IMPLEMENTATIONS AND MEASUREMENT RESULTS

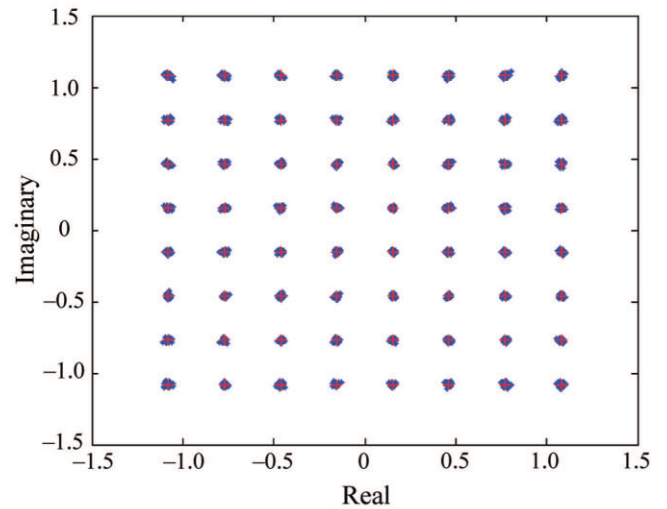
To investigate the proposed algorithm for the linearization of a wideband signal, we have employed a 2.655-GHz mobile WiMAX 2FA signal with 20-MHz bandwidth and 8.4 dB PAPR at the 0.01% level of the CCDF. Here, the peak level of the original signal with more than 10-dB PAPR is reduced by the CFR technique so that the EVM is disturbed; relative constellation error (RCE) of the employed signal is about -39 dB. For the linearization test, a class-AB amplifier is built using two Freescale MRF6S27085 LDMOSFETs with 85-W PEP. The Agilent Advanced Design System using an electronic signal generator and vector signal analyzer connected solution is used for the test [13].



(a)



(b)



(c)

**Figure 7** Measured constellation diagram before and after linearizations at an average output power of 42 dBm. (a) Without predistorter. (b) Digital feedback predistorter. (c) Wideband digital feedback predistorter. [Color figure can be viewed in the online issue, which is available at [www.interscience.wiley.com](http://www.interscience.wiley.com)]

The proposed algorithm has two 512-entry AM/AM and AM/PM LUTs and the memory compensation structure of  $Q = 2$  and  $L = 7$  presented in (1), which are programmed by MATLAB using the DFBDP and RLS algorithms, respectively. The capability of the proposed algorithm is evaluated by linearizing the implemented amplifier exhibiting serious memory effects and comparing with the DFBDP algorithm.

Figure 2 illustrates IMD3 and IMD5 of the PA for the two-tone signals up to 20-MHz tone spacing. This amplifier exhibits serious memory effects as presented in the differences between the upper and lower levels of IMD3 and IMD5. This IMD3 difference has a maximum value of 21 dB at an average output power of 47 dBm. Figure 3 shows the AM/AM and AM/PM characteristics before linearization and after predistortion by the DFBDP and WDFBDP algorithms. The DFBDP algorithm provides the memoryless PD signal, while the WDFBDP algorithm generates the memory PD signal that linearizes the instantaneous nonlinearity of the PA. The PD signal produced by the WDFBDP algorithm assures that the memory compensation is properly combined with the DFBDP linearization algorithm. Figure 4(a) shows the measured spectrum of the amplifier. The amplifier generates lower spurious emission in the lower band than in the upper band for the WiMAX 2FA signal. Figure 4(b) shows the measured spectra of the PD signals generated by the algorithms. The DFBDP algorithm provides balanced spurious emission, while the WDFBDP algorithm generates unbalanced spurious emission to compensate the memory effects.

Figure 5 shows the measured AM/AM and AM/PM characteristics at the amplifier output after DFBDP and WDFBDP linearizations at an average output power of 42 dBm. The nonlinear characteristics are successfully linearized by both linearization algorithms. However, the AM/AM and AM/PM scattering is suppressed better by the WDFBDP linearization. Figure 6 shows the measured WiMAX 2FA spectra before and after DFBDP and WDFBDP linearizations at the same average output power. The ACLR at an offset of 7.144-MHz for the WDFBDP algorithm is  $-51.5$  dBc, which is an improvement of about 19 dB at the same average output power. Figure 7 shows the measured constellation diagram before and after DFBDP and WDFBDP linearizations at an average output power of 42 dBm. The RCE is  $-38.2$  dB, an improvement of about 8.5 dB. In comparison with the DFBDP algorithm, the WDFBDP algorithm delivers for better linearization because of the memory-effect compensation. The measured linearization results are summarized in Table 1.

#### 4. CONCLUSIONS

We have presented a new DFBDP technique that combines the DFBDP with the memory polynomial structure. The algorithm provides highly efficient nonlinearity compensation by the DFBDP method, and the memory polynomial becomes very simplified, requiring only a second-order nonlinearity and seven memory taps. For a 2.655-GHz mobile WiMAX 2FA signal with 20-MHz bandwidth, the proposed WDFBDP technique provides an ACLR at

7.144-MHz offset and RCE of the amplifier of  $-51.5$  dBc and  $-38.2$  dB, which are improvements of about 19 dB and 8.5 dB, respectively, at an average output power of 42 dBm. We have demonstrated that the DFBDP technique is possible to combine with other structures, so that the proposed WDFBDP technique delivers better linearization performance for the WiMAX signal, while maintaining most of the DFBDP technique's advantages. We believe that the WDFBDP technique is suitable to linearize PAs for the mobile WiMAX multicarrier application.

#### ACKNOWLEDGMENT

This work was supported by the Ministry of Knowledge Economy, Korea, under the Information Technology Research Center (ITRC) support program supervised by the Institute of Information Technology Advancement (IITA-2008-C1090-0801-0037), and partially sponsored by ETRI SoC Industry Promotion Center, Human Resource Development Project for IT SoC Architect. The authors thank the Telecommunication Research and Development Center, Samsung Electronics Company Ltd., for supplying the 802.16e mobile WiMAX signal used in this study.

#### REFERENCES

1. "Framework and overall objectives of the future development of IMT-2000 and systems beyond IMT-2000 in Recommendation ITU-R M.1645," 2003.
2. M. Steer, Beyond 3G, IEEE Microwave Mag 8 (2007), 76–82.
3. L. Ding, G.T. Zhou, D.R. Morgan, Z. Ma, J.S. Kenney, J. Kim, and C.R. Giardina, A robust digital baseband predistorter constructed using memory polynomials, IEEE Trans Commun 52 (2004), 159–165.
4. L. Ding, Z. Ma, D.R. Morgan, M. Zierdt, and J. Pastalan, A least-squares/Newton method for digital predistortion of wideband signals, IEEE Trans Commun 54 (2006), 833–840.
5. T. Liu, S. Boumaiza, and F.M. Ghannouchi, Deembedding static nonlinearities and accurately identifying and modeling memory effects in wide-band RF transmitters, IEEE Trans Microwave Theory Tech 53 (2005), 3578–3587.
6. D.R. Morgan, Z. Ma, J. Kim, M.G. Zierdt, and J. Pastalan, A generalized memory polynomial model for digital predistortion of RF power amplifiers, IEEE Trans Signal Process 54 (2006), 3852–3860.
7. T. Liu, S. Boumaiza, and F.M. Ghannouchi, Augmented Hammerstein predistorter for linearization of broad-band wireless transmitters, IEEE Trans Microwave Theory Tech 54 (2006), 1340–1349.
8. Y. Kim, Y. Yang, S. Kang, and B. Kim, Linearization of 1.85 GHz amplifier using feedback predistortion loop, In: IEEE MTT-S Int Microwave Symp Dig, 1998, pp. 1675–1678.
9. Y.Y. Woo, J. Kim, J. Yi, S. Hong, I. Kim, J. Moon, and B. Kim, Adaptive digital feedback predistortion technique for linearizing power amplifiers, IEEE Trans Microwave Theory Tech 55 (2007), 932–940.
10. Y.Y. Woo, J. Kim, S. Hong, I. Kim, J. Moon, J. Yi, and B. Kim, A new adaptive digital predistortion technique employing feedback technique, In: IEEE MTT-S Int Microwave Symp Dig, June 2007, pp. 1445–1448.
11. J. Kim, Y.Y. Woo, J. Moon, and B. Kim, A new wideband adaptive digital predistortion technique employing feedback linearization, IEEE Trans Microwave Theory Tech 56 (2008), 328–338.
12. S. Haykin, Adaptive filter theory, Prentice-Hall, Upper Saddle River, NJ, 2001.
13. Connected simulation and test solutions using the advanced design system, Application Note 1394, Agilent Technologies, Palo Alto, CA, 2000.

© 2008 Wiley Periodicals, Inc.

**TABLE 1 Measured Performance Before and After Linearizations at an Average Output Power of 42 dBm for WiMAX 2FA Signal**

	ACLR (dBc) at $-/+$	
	7.144-MHz	RCE (dB)
Amplifier	$-37.3/-32.6$	$-29.8$
DFBDP + Amp.	$-45.0/-48.4$	$-35.9$
WDFBDP + Amp.	$-53.2/-51.5$	$-38.2$